

# Optimization of preselection for bb/cc/ss studies at ILC250 ( $2000 \text{ fb}^{-1}$ ) with the ILD

Jesús Pedro Márquez Hernández  
Adrian Irles Quiles  
*IFIC – CSIC – UV*

16/06/2021

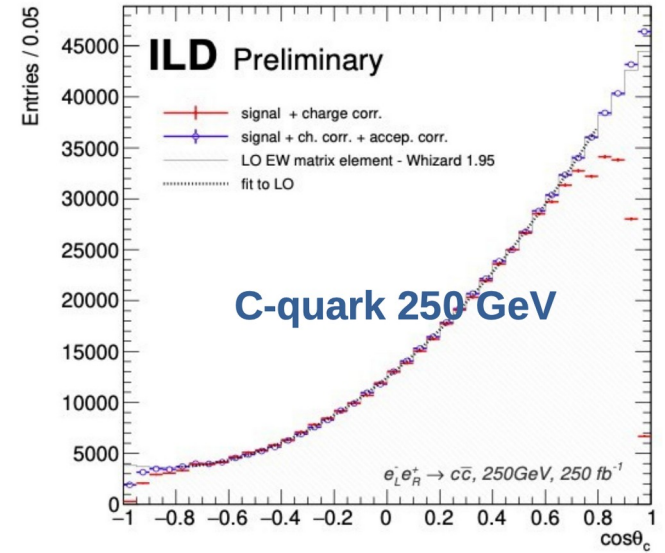
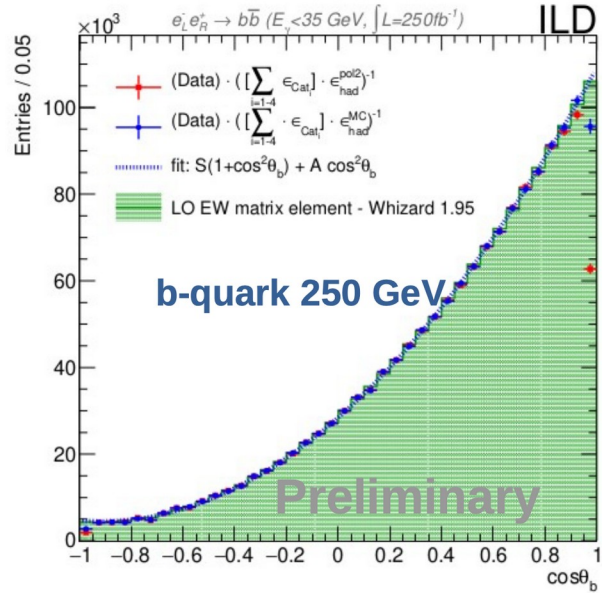
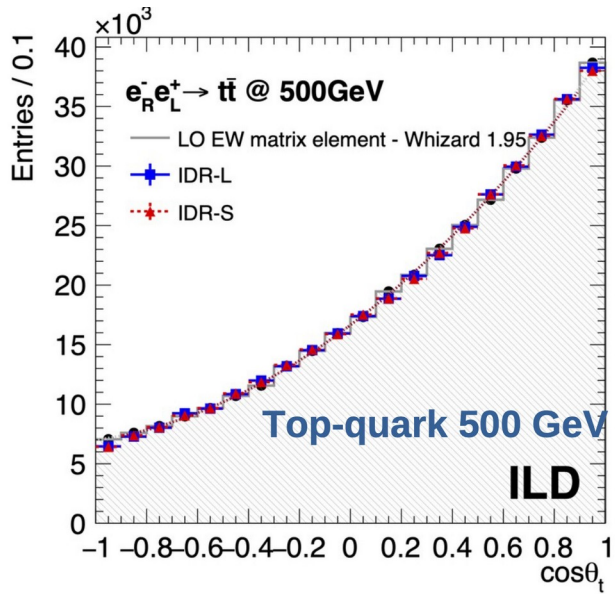


# Realistic studies with full simulation

ILD Note  
(Okugawa et al)

Preliminary Results  
Presented in several conferences  
(Irles, Poeschl, Richard)  
Draft for publication in progress

Preliminary Results  
Presented in LCWS19 (and others)  
(Irles et al)  
More detailed analysis in progress



The study presented here defines the preselection for all new ss/cc/bb studies at  $\sqrt{s} = 250$  GeV and will define the starting point for  $\sqrt{s}=500$  GeV samples

ss-quark study going on (Okugawa)

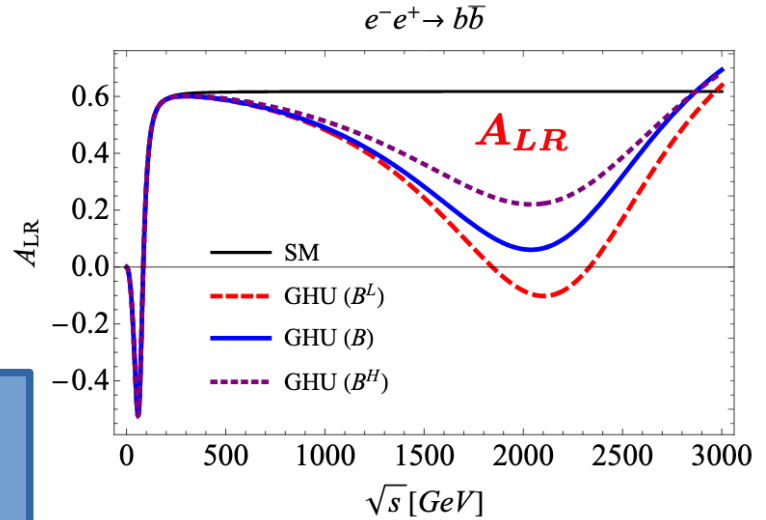
# Global strategy

Research team:  
 Instituto de Física Corpuscular (IFIC)  
 and  
 Irène Joliot-Curie Lab (IJCLab)

Potential for studying BSM physics  
 (e.g. Hosotani's GHU Model)



For a deep and complete study of the quark EW couplings (SM and BSM) we need to study different flavors and run at different energies ( $\sqrt{s}=91, 250, 500$  GeV)



# My study: Introduction

Data analysis of ILC simulated data:

- Final goal: Studying b-quark EW couplings.
  - Observables:  $R_b^{cont}$ ,  $\frac{d\sigma}{d\cos\theta_b}$  and  $A_{FB}^{b\bar{b}}$
- Data processed with the VLC algorithm:
  - Pfos are ordered in 2 jets
    - For the signal we expect the two jets in back-to-back topology (but not for the background)
- Most of the background is radiative return
  - And most of the data is background! (x3 for  $e_L^-e_R^+$  and x6 for  $e_R^-e_L^+$ )
- Event preselection procedure:
  - Cut in radiative returns
  - Cut in background from pair of heavy bosons

We need a preselection with homogeneous efficiency in the volume of the detector and with minimal flavor dependence: to avoid modeling uncertainties (see, for example, [Irlles talk](#))

# Results before 2020 (I)

Results from the DBD samples:

- Cuts:
  - $K_{reco} < 35 \text{ GeV} \ \& \ m_{2jets} > 130 \text{ GeV}$
  - $N \text{ pfos} > 5$
  - Photo vetoing (100, 70)
  - $y_{23} < 0.015$
  - $m_{j1} + m_{j2} < 100 \text{ GeV}$
- Efficiencies:

Efficiency (%)			
$b\bar{b}$	$c\bar{c}$	$q\bar{q}(uds)$	ISR
71.5	71.1	70.7	0.7

Table 1: Total efficiency of the preselection for the different quark flavors and radiative return (DBD samples)

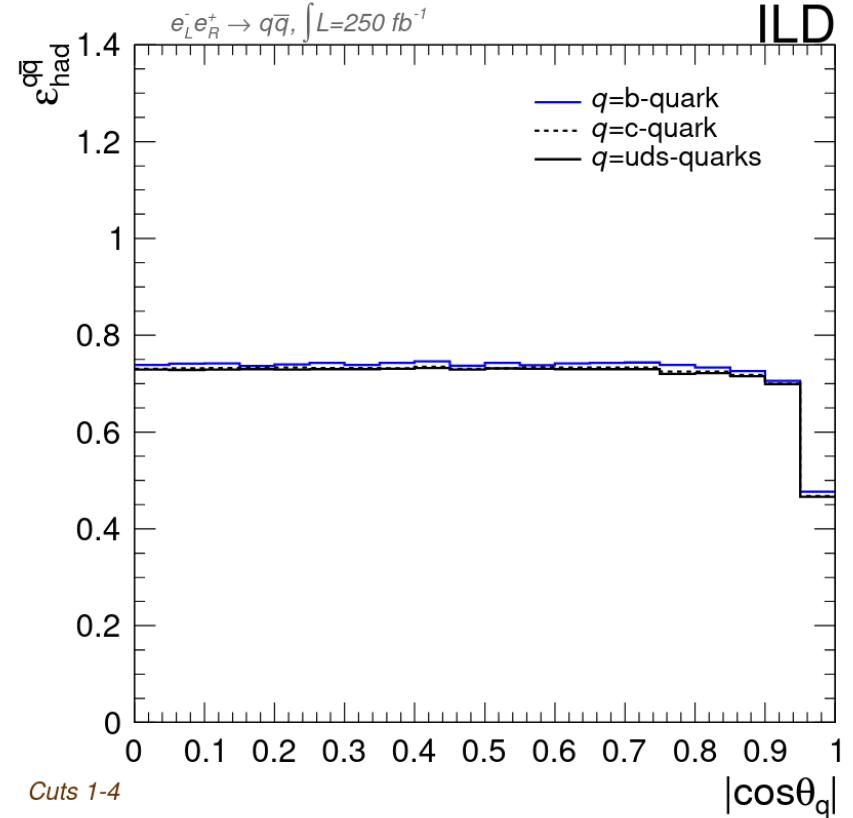


Fig. 1: Efficiency of the preselection for the different quark flavors vs the angular distribution of the two jet system (DBD samples)

- Aim:
  - Obtaining maximal, uniform and flavor non-dependent efficiency
  - Lowest background possible

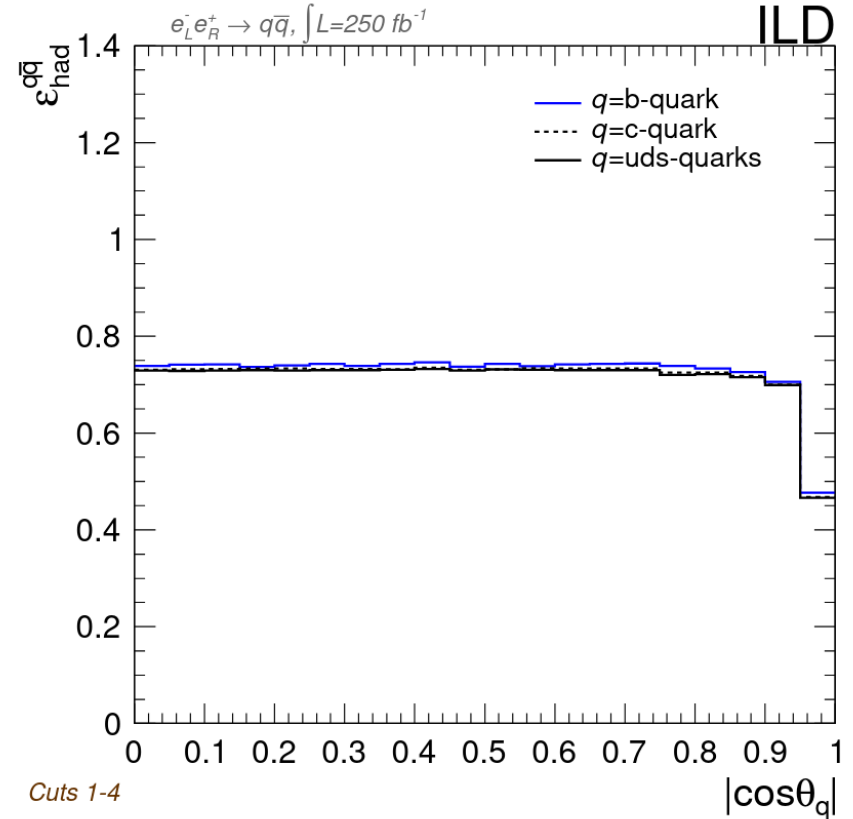


Fig. 1: Efficiency of the preselection for the different quark flavors vs the angular distribution of the two jet system (DBD samples)

# New samples

Results from the new samples applying DBD designed cuts:

- Cuts:
  - $K_{reco} < 35 \text{ GeV} \ \& \ m_{2jets} > 130 \text{ GeV}$
  - N pfos > 5
  - Photon veto
  - $y_{23} < 0.015$
  - $m_{j1} + m_{j2} < 100 \text{ GeV}$

Efficiencies:

Efficiency (%)			
$b\bar{b}$	$c\bar{c}$	$q\bar{q}(uds)$	ISR
71.5	69.9	68.4	0.7

Table 2: Total efficiency of the preselection for the different quark flavors and radiative return (new samples applying DBD designed cuts)

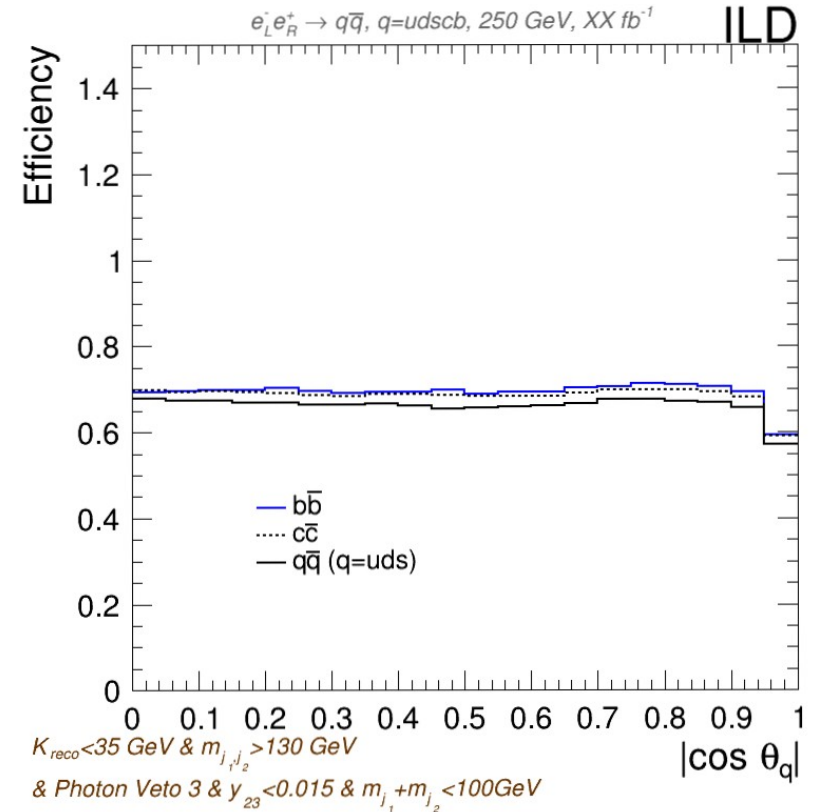


Fig. 2: Efficiency of the preselection for the different quark flavors vs the angular distribution of the two jet system (new samples applying DBD designed cuts)

# New samples

Results from the new samples applying DBD designed cuts::

- Cuts:
  - $K_{reco} < 35 \text{ GeV} \ \& \ m_{2jets} > 130 \text{ GeV}$
  - N pfos > 5
  - Photon veto
  - $y_{23} < 0.015$
  - $m_{j_1} + m_{j_2} < 100 \text{ GeV}$

Efficiencies:

	$E_{jet} > 70$		
$b\bar{b}$	$c\bar{c}$	$q\bar{q}(uds)$	ISR
71.5	69.9	68.4	0.7

Table 2: Total efficiency of the preselection for the different quark flavors and radiative return (new samples applying DBD designed cuts)

This preselection creates differences between flavors

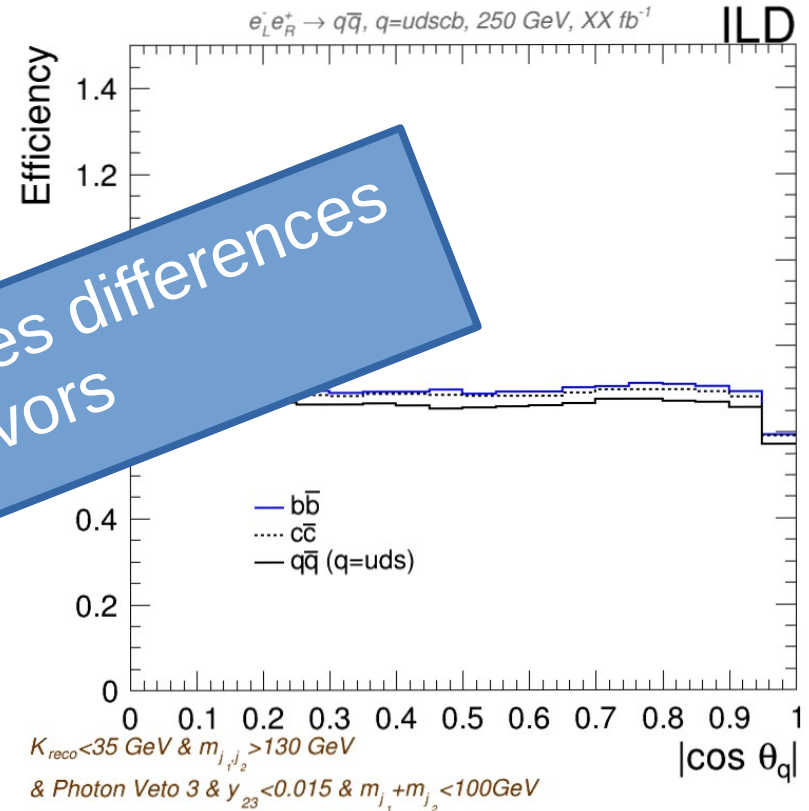


Fig. 2: Efficiency of the preselection for the different quark flavors vs the angular distribution of the two jet system (new samples applying DBD designed cuts)



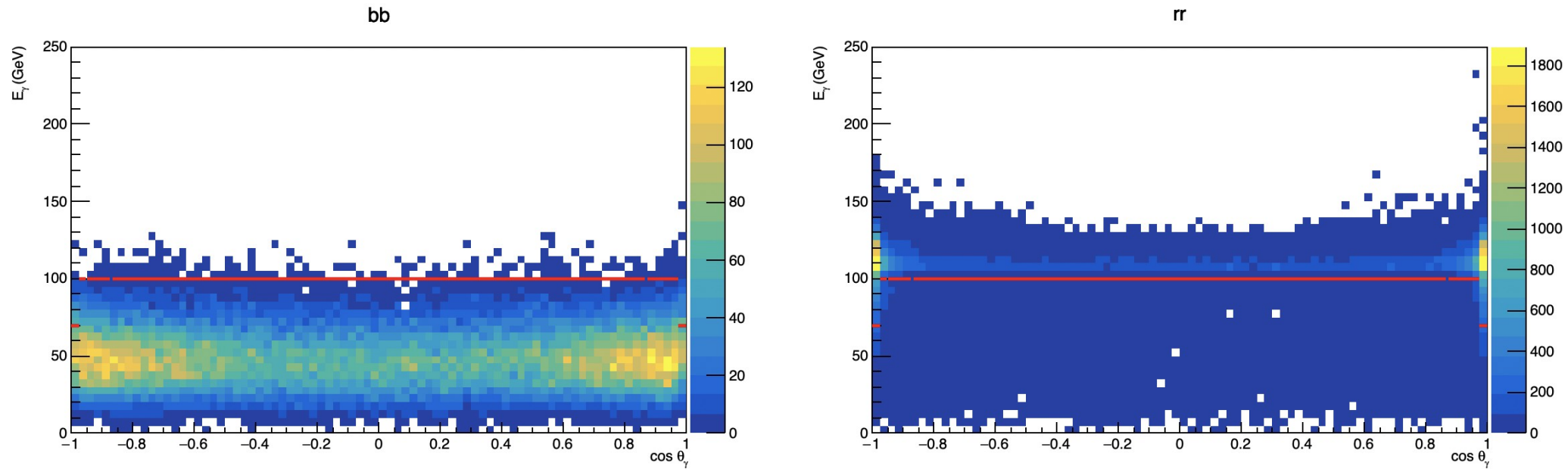


Fig. 3: Two dimensional maps used for the photon vetoing; impact in different quark flavors (new samples). Left plot is for b-quark events while the right plot is for ISR. The y-axis is the energy (GeV) of the pfos identified as photons by the jet reconstruction algorithm and the x-axis is  $\cos(\theta)$  of those pfos.

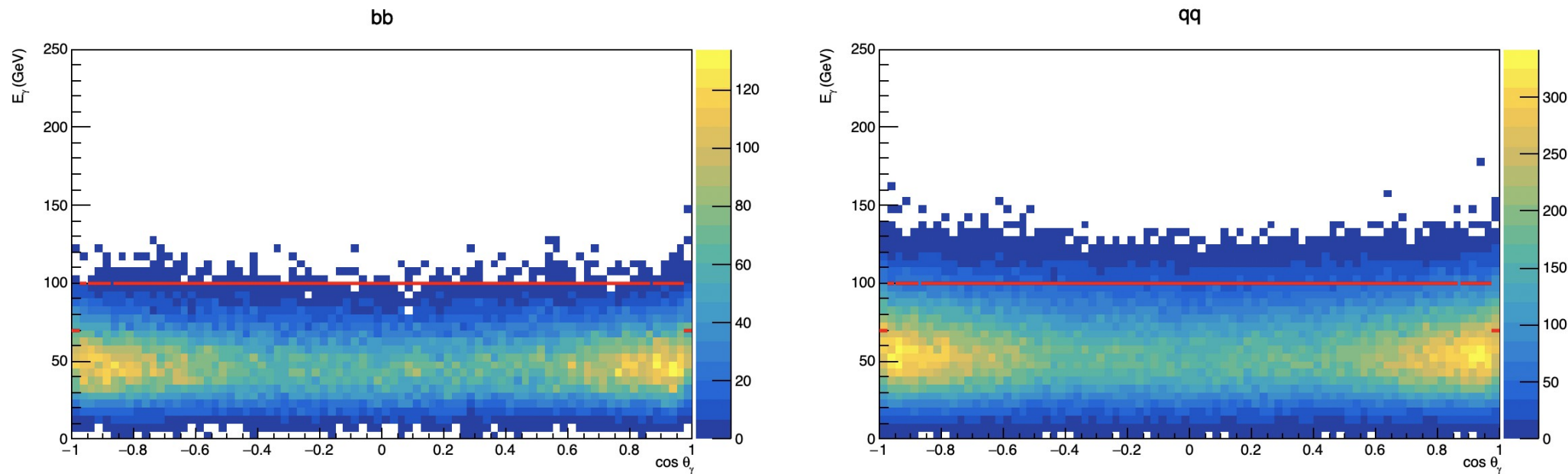


Fig. 4: Two dimensional maps used for the photon vetoing; impact in different quark flavors (new samples). Left plot is for b-quark events while the right plot is for uds-quarks. The y-axis is the energy (GeV) of the pfos identified as photons by the jet reconstruction algorithm and the x-axis is  $\cos(\theta)$  of those pfos.

If we try to re-balance the selection efficiencies by leveling up these energies levels then the rejection efficiency for the radiative return goes all the way up to  $\sim 2\%$

Next step:  
Re-optimization of the cuts

# Re-optimization of the cuts: $K_{reco}$

- $K_{reco}$  is a good estimator of  $E_\gamma$ :
  - Definition of acolinearity:

$$\sin \Psi_{acol} = \frac{|\vec{p}_{j_1} \times \vec{p}_{j_2}|}{|\vec{p}_{j_1}| \cdot |\vec{p}_{j_2}|}$$

- Momentum of the collinear photon in the ultrarelativistic limit ( $m_{jets} \ll p_{jets}$ ):

$$|\vec{k}| \approx K_{reco} = \frac{250 \text{ GeV} \cdot \sin \Psi_{acol}}{\sin \Psi_{acol} + \sin \theta_1 + \sin \theta_2}$$

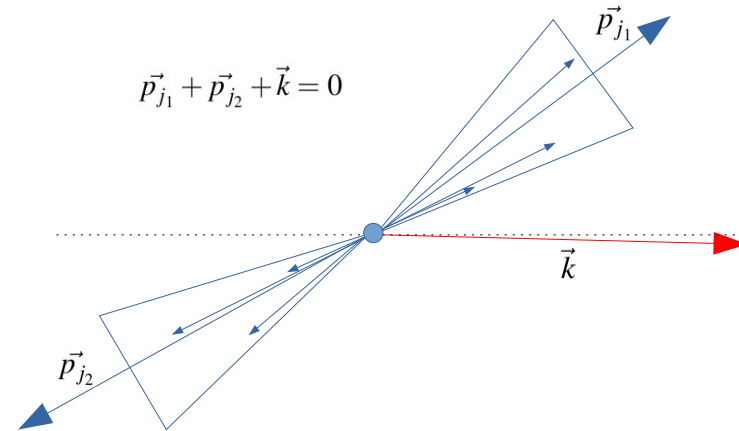
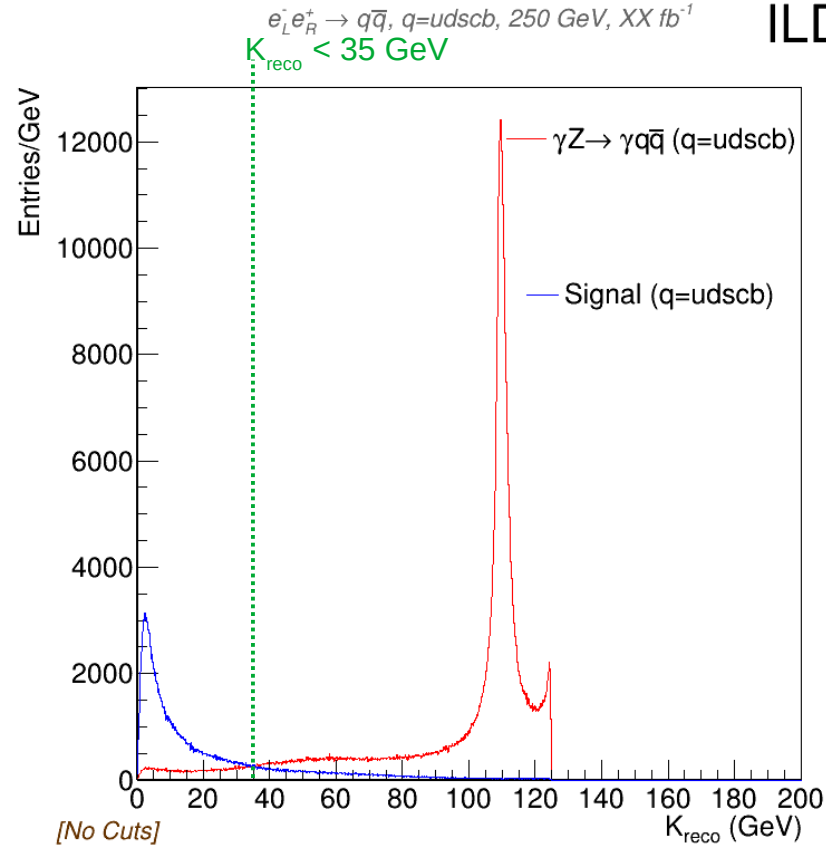


Fig. 5: Kinematics of a two jets system reconstruction with ISR

# Re-optimization of the cuts: $K_{\text{reco}}$ (II)



We set the cut to  
 $K_{\text{reco}} < 35 \text{ GeV}$

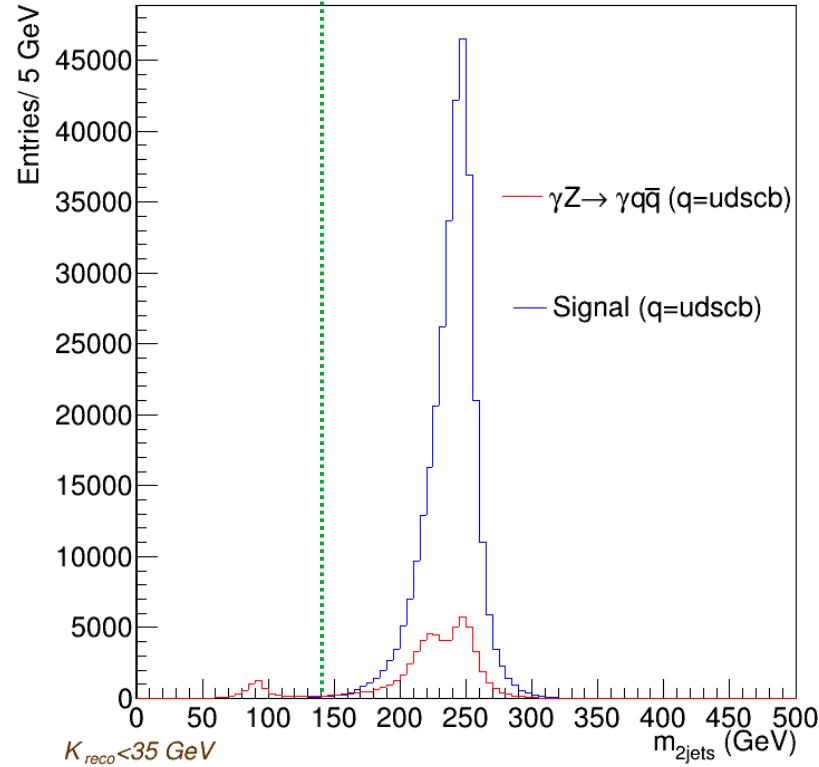
Fig. 6: Distribution of events vs  $K_{\text{reco}}$ . The green vertical lines represent the different cuts tried for  $K_{\text{reco}}$

# Re-optimization of the cuts: $m_{2\text{jets}}$

$e_L^- e_R^+ \rightarrow q\bar{q}$ ,  $q=uds\text{cb}$ , 250 GeV,  $XX \text{ fb}^{-1}$   
 $m_{2\text{jets}} > 140$

ILD

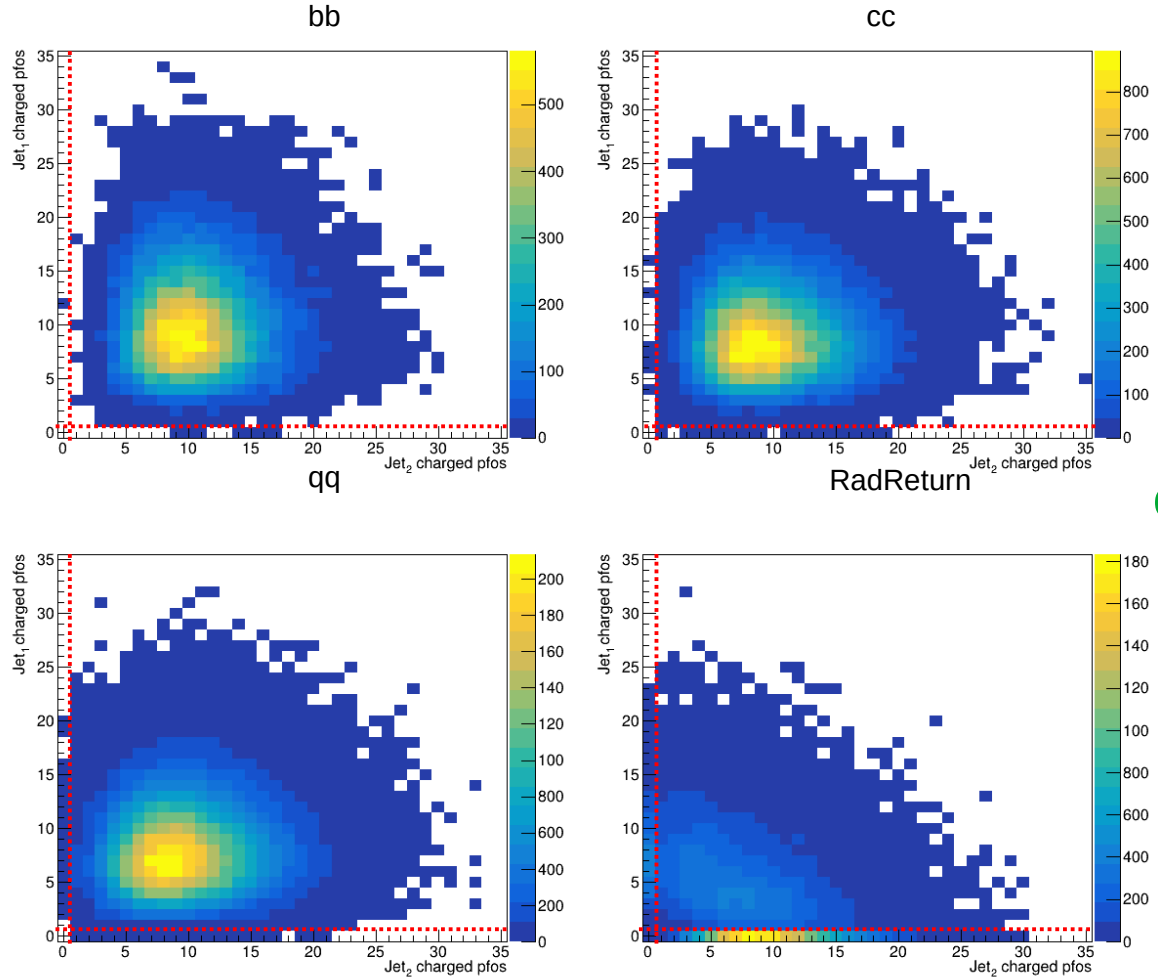
$m_{2\text{jets}}$  is the sum of the masses of both jets



We set the cut to  $m_{2\text{jets}} > 140 \text{ GeV}$

Fig. 7: Distribution of events vs  $m_{2\text{jets}}$ . The green vertical line represents the selected cut for  $m_{2\text{jets}}$ .

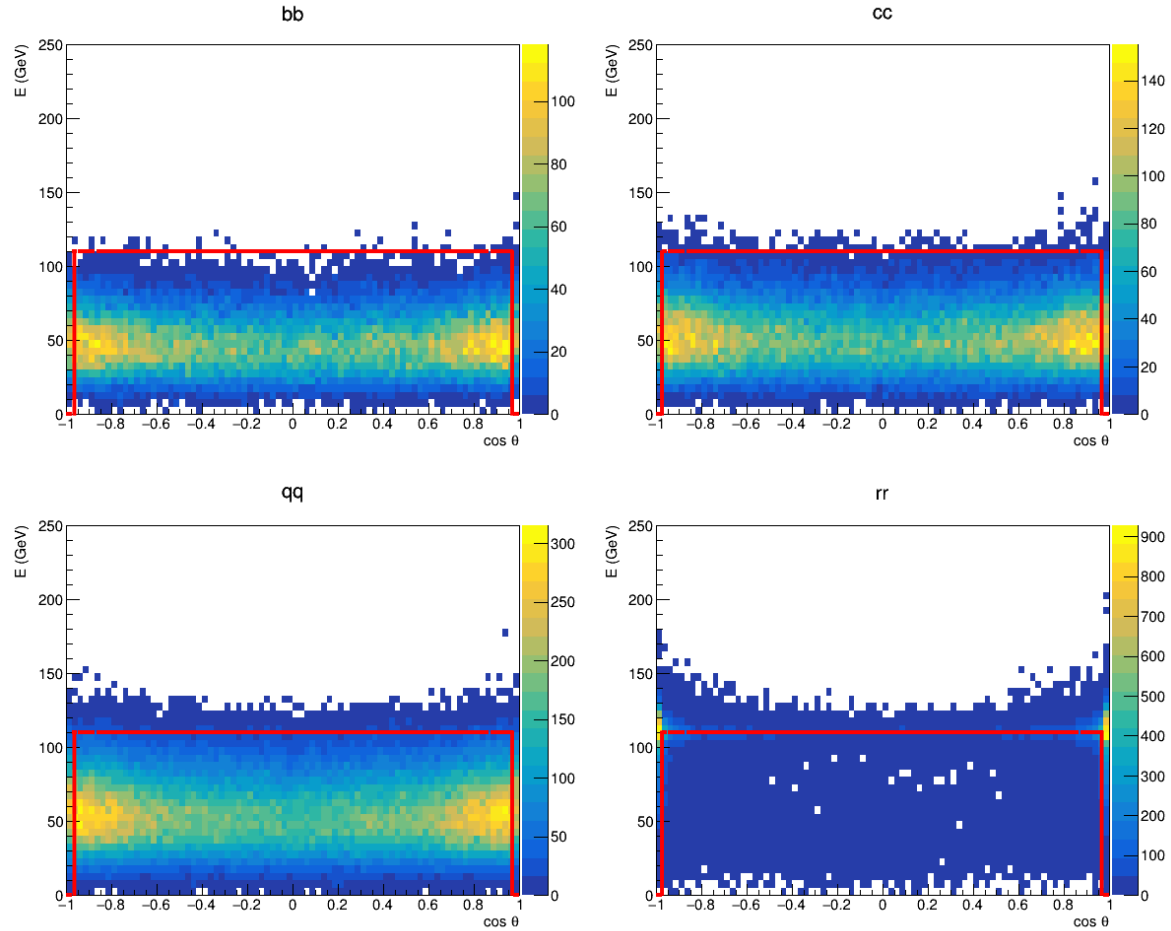
# Re-optimization of the cuts: Charged PFOs



At least 1  
charged pfo  
in each jet

Fig. 8: Selected cut for the number of charged ppos associated to each jet

# Re-optimization of the cuts: Photon veto



$E > 110 \text{ GeV}$   
and  
 $|\cos\theta| < 0.97$

Fig. 9: Selected cut for the angular distribution of energy (photon vetoing)



# Re-optimization of the cuts: Overview

## Previous approach:

- Cuts:
  - $K_{reco} < 35 \text{ GeV} \ \& \ m_{2jets} > 130 \text{ GeV}$
  - $N \text{ pfos} > 5$
  - Photon veto (DBD cuts)
  - $y_{23} < 0.015$
  - $m_{j1} + m_{j2} < 100 \text{ GeV}$

## Efficiencies:

Efficiency (%)			
$b\bar{b}$	$c\bar{c}$	$q\bar{q}(uds)$	ISR
71.5	69.9	68.4	0.7

Table 3: Total efficiency of the preselection for the different quark flavors and radiative return with the previous cut selection (new samples)

## New approach:

- Cuts:
  - $K_{reco} < 35 \text{ GeV}$
  - $m_{2jets} > 140 \text{ GeV}$
  - Charged pfos  $> 1$
  - Photon veto (previous slide)
  - $Y_{23} < 0.015$  (we kept this unchanged)

## Efficiencies:

Efficiency (%)			
$b\bar{b}$	$c\bar{c}$	$q\bar{q}(uds)$	ISR
68.4	68.4	68.0	1.2

Table 4: Total efficiency of the preselection for the different quark flavors and radiative return with the new cut selection (new samples)

Better but not good enough :/

After optimizing the cuts, we tried to optimize the performance of the jet reconstruction algorithm

# Re-optimization of the cuts: VLC algorithm

- Definitions

$$d_{ij} = 2 \min(E_i^{2\beta}, E_j^{2\beta}) (1 - \cos \theta_{ij}) / R^2,$$

$$d_{iB} = E_i^{2\beta} \sin^{2\gamma} \theta_{iB},$$

- We played with the parameters R and  $\gamma$ :

- R: (0.50, 0.96, 1.00, 1.05, 1.17, 1.28, 1.36, 1.68)
- $\gamma$ : (0.0, 0.5, 1.0)

- We kept  $\beta=1$

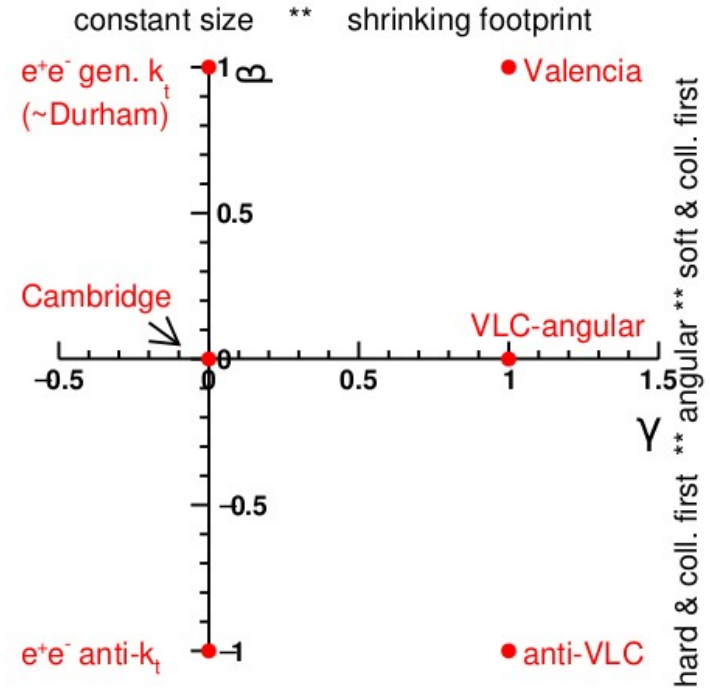


Fig. 10: Diagram of the parameter space spanned by exponents  $\gamma$  and  $\beta$ . [1]

# Re-optimization of the cuts: VLC algorithm – R (I)

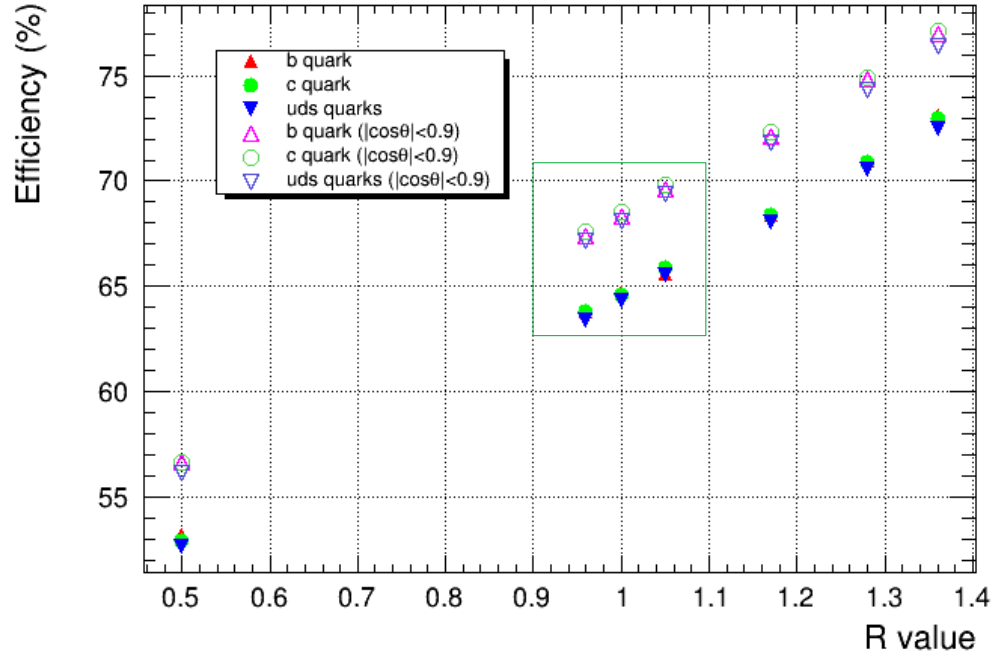


Fig. 11: Selection efficiencies for different quark flavors and R values (with and without angular restriction)

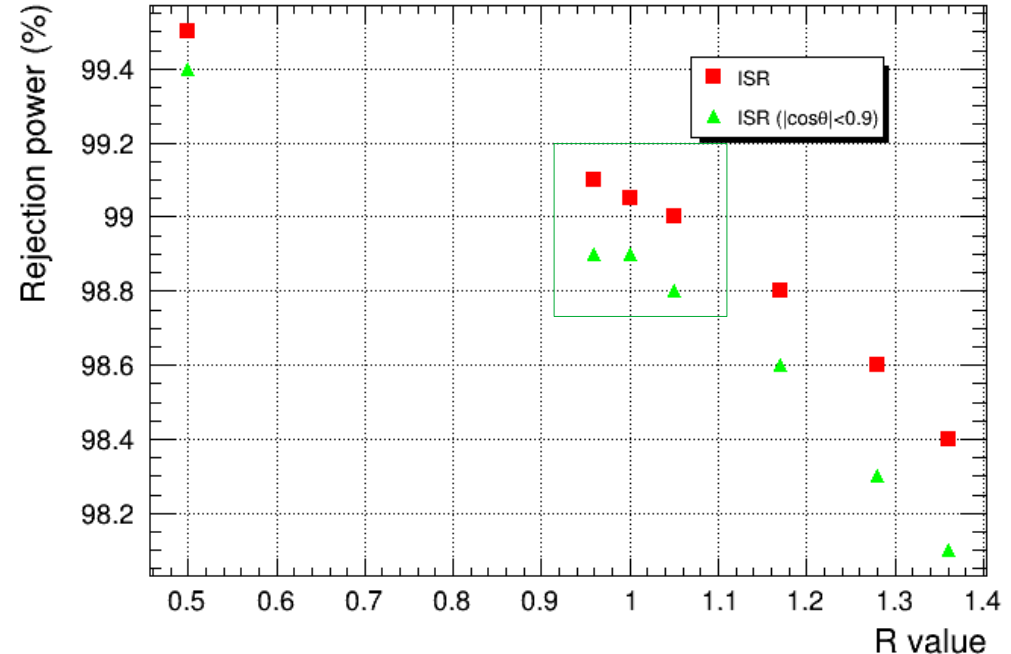


Fig. 12: Rejection power for different R values (with and without angular restriction)

# Re-optimization of the cuts: VLC algorithm – R (II)

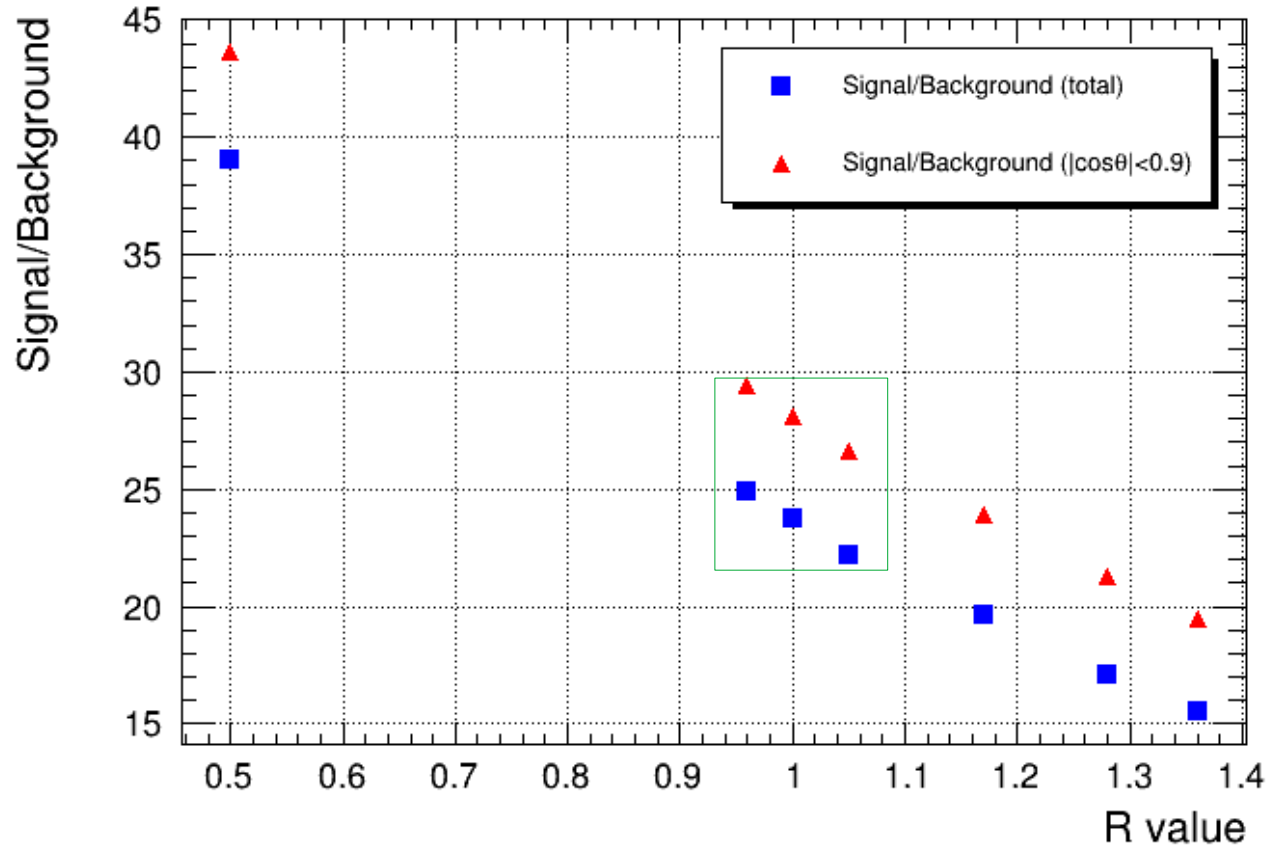
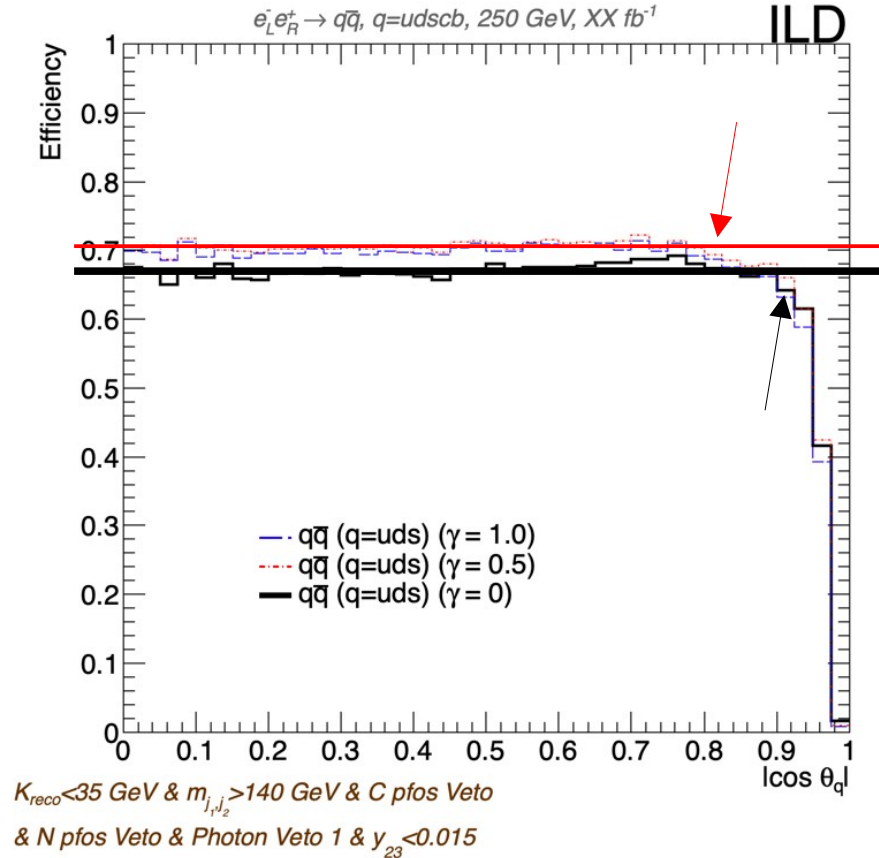


Fig. 13: Signal/Background for different values of R (with and without angular restriction)

# Re-optimization of the cuts: VLC algorithm – $\gamma$

- Impact in the very forward/backward regions:



Smaller  $\gamma$  provide slightly smaller global efficiencies but more homogeneous efficiencies in most of the detector volume ( $|\cos(\theta)| < 0.9$ )

The best parameter choices are  $R=1$  and  $\gamma=0$ .

Fig. 14: Efficiency of the preselection for light quarks (uds) vs the angular distribution of the two jet system. Plots with  $R=1$  and  $\gamma=0.0, 0.5$  and  $1.0$

# Conclusions

- A new optimization of the preselection is provided. This is to be used in ss/cc/bb analysis at  $\sqrt{s}=250\text{GeV}$  and will be the starting point for  $\sqrt{s}=500\text{GeV}$
- At higher energies, the VLC algorithm may play a more important role (larger beam background expected)
- Chosen configuration:

<p><b>Cuts:</b></p> <ul style="list-style-type: none"> <li>• <math>K_{reco} &lt; 35 \text{ GeV}</math></li> <li>• <math>m_{2jets} &gt; 140 \text{ GeV}</math></li> <li>• Charged N pfos</li> <li>• Photon veto</li> <li>• <math>Y_{23} &lt; 0.015</math></li> </ul>	<p><b>VLC Algorithm parameters:</b></p> <ul style="list-style-type: none"> <li>• <math>R = 1.0</math></li> <li>• <math>\gamma = 0.0</math></li> <li>• <math>\beta = 1.0</math></li> </ul>
---	---

R	Efficiencies (%)			ISR	S/B
	$b\bar{b}$	$c\bar{c}$	$q\bar{q}$ (uds)		
1.0	64.7	64.6	64.3	0.9	23.7
	68.3	68.5	68.1	1.1	28.1

←  $|\cos\theta| < 0.9$

Table 5: Total efficiency of the preselection for the different quark flavors and radiative return for the chosen configuration ( $\gamma=0$ ). The second row is for  $|\cos\theta| < 0.9$

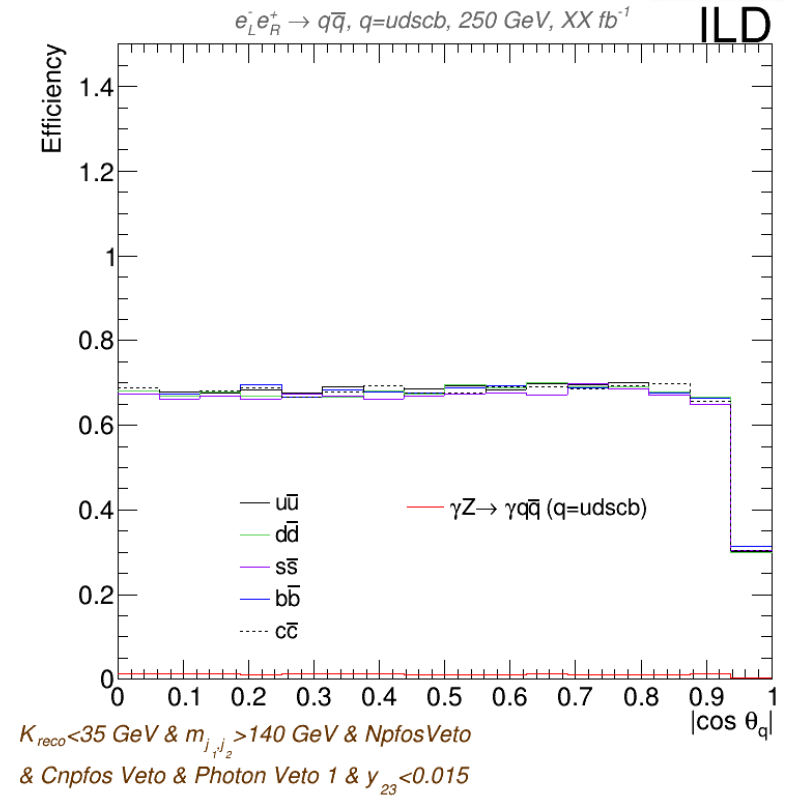


Fig. 15: Efficiency of the preselection for the different quark flavors vs the angular distribution of the two jet system (new samples, final configuration)

# END OF THE PRESENTATION

THANKS FOR YOUR ATTENTION

Jesús P. Márquez Hernández



# BACK-UP SLIDES

# Re-optimization of the cuts: Why do we need equal efficiencies?

- Impact in the Double Tag method for b-tagging:

- Observables:

- Ratio of q-flavored quarks:

$$R_q^{cont.}(|\cos\theta_q|) = \frac{\sigma_{e^-e^+ \rightarrow q\bar{q}}^{cont.}(|\cos\theta|)}{\sigma_{had.}^{cont.}(|\cos\theta|)}$$

For a specific q flavor

All possible q flavors

Having different selection efficiencies for each quark flavor will lead to a biased computation of this observable

This bias affects the b-tagging process

- Fraction of jets tagged as b-quark (first tag):

$$f_1 = \epsilon_b R_b^{cont.} + \epsilon_c R_c^{cont.} + \epsilon_{uds}(1 - R_b^{cont.} - R_c^{cont.}) + F_1^{bkg}(\epsilon_c, \epsilon_b, \epsilon_{uds}, BKG)$$

- Fraction of preselected events in which both jets are tagged as b-quark (second tag):

$$f_2 = \epsilon_b^2(1 + \rho_b)R_b^{cont.} + \epsilon_c^2 R_c^{cont.} + \epsilon_{uds}^2(1 - R_b^{cont.} - R_c^{cont.}) + F_2^{bkg}(\epsilon_c^2, \epsilon_b^2, \epsilon_{uds}^2, BKG)$$

# Re-optimization of the cuts: Leveling up the photon veto

## Previous approach:

- Cuts:
  - $K_{reco} < 35 \text{ GeV} \ \& \ m_{2jets} > 130 \text{ GeV}$
  - $N \text{ pfos} > 5$
  - Photon vetoing
  - $y_{23} < 0.015$
  - $m_{j1} + m_{j2} < 100 \text{ GeV}$

## Efficiencies:

Efficiency (%)			
$b\bar{b}$	$c\bar{c}$	$q\bar{q}(uds)$	ISR
71.5	69.9	68.4	0.7

Table E1: Total efficiency of the preselection for the different quark flavors and radiative return with the previous cut selection (new samples)

## Re-balancing the photon veto:

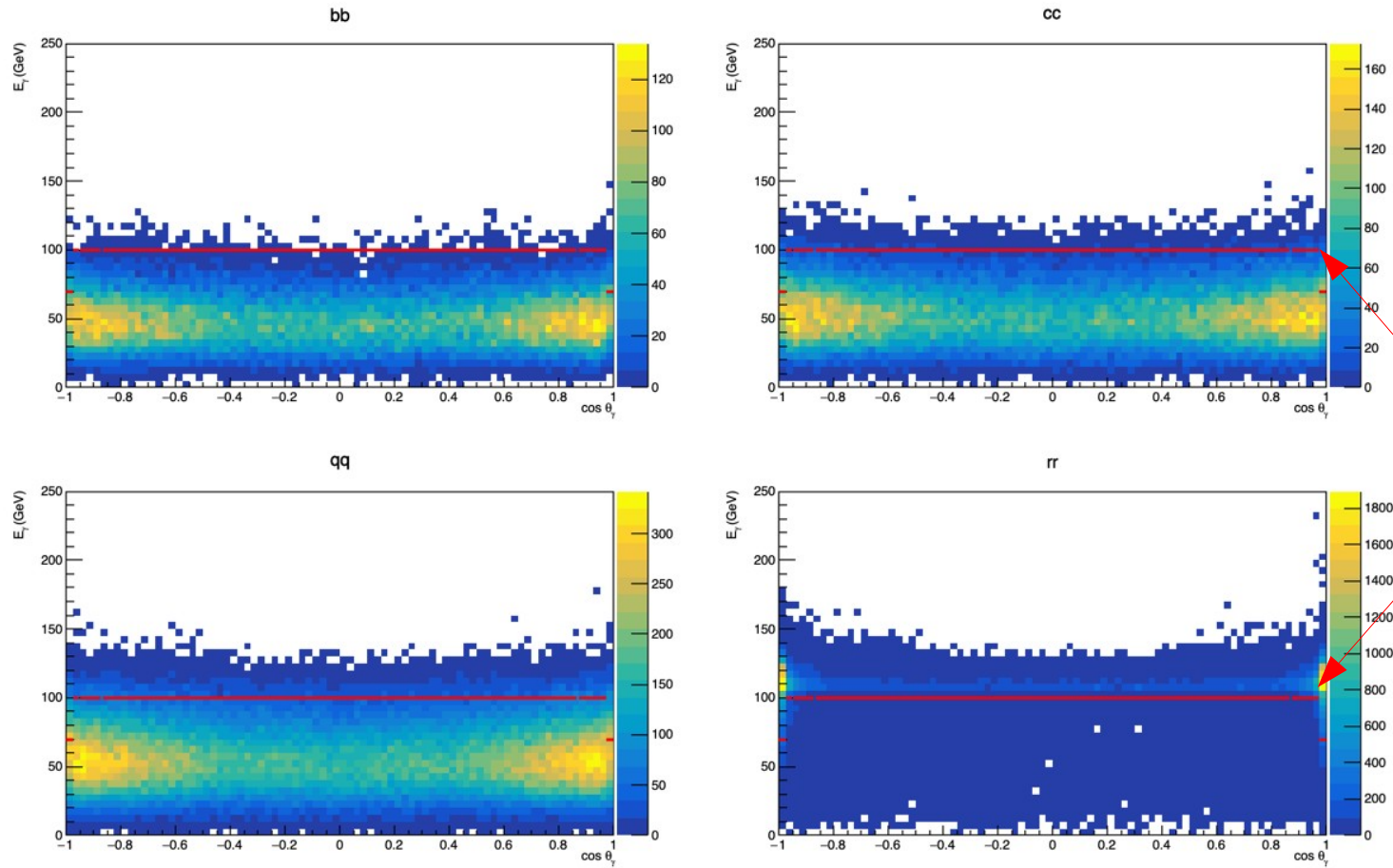
- Cuts:
  - $K_{reco} < 35 \text{ GeV} \ \& \ m_{2jets} > 130 \text{ GeV}$
  - $N \text{ pfos} > 5$
  - Photon vetoing (leveling up)
  - $y_{23} < 0.015$
  - $m_{j1} + m_{j2} < 100 \text{ GeV}$

## Efficiencies:

Efficiency (%)			
$b\bar{b}$	$c\bar{c}$	$q\bar{q}(uds)$	ISR
71.2	71.1	71.0	1.9

Table E2: Total efficiency of the preselection for the different quark flavors and radiative return with the new cut selection (new samples)

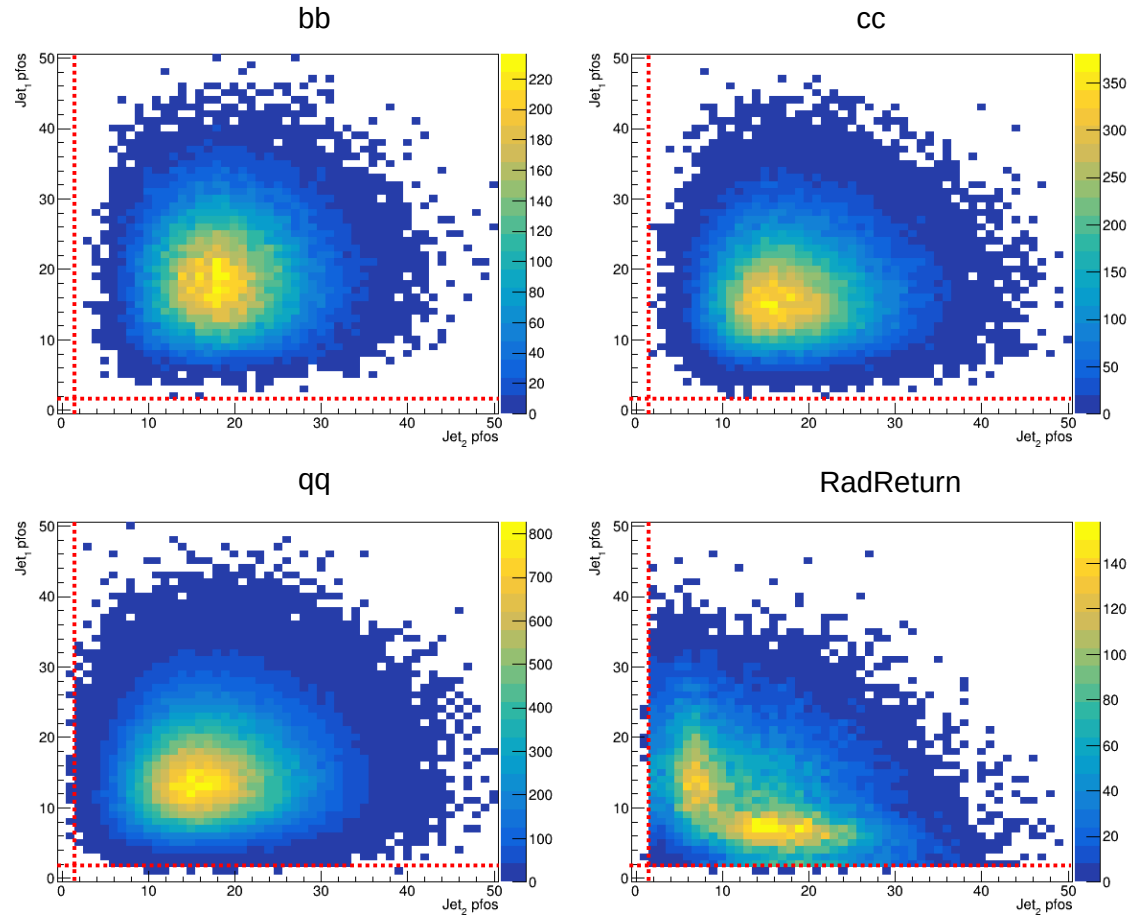
# New samples (Photon veto)



If we try to re-balance the selection efficiencies by leveling up these energies levels then the rejection efficiency for the radiative return goes up to  $\sim 2\%$

Fig. E1: Two dimensional maps used for the photon vetoing; impact in different quark flavors (new samples). The y-axis is the energy (GeV) of the pfos identified as photons by the jet reconstruction algorithm and the x-axis is  $\cos(\theta)$  of those pfos.

# Re-optimization of the cuts: N. PFOs



At least 2  
pfos in each  
jet

Fig. E2: Selected cut for the number of total pfos associated to each jet

# Re-optimization of the cuts: VLC algorithm – $\gamma$ (E. I)

R	Efficiency (%)											
	$\gamma = 0.0$				$\gamma = 0.5$				$\gamma = 1.0$			
	$b\bar{b}$	$c\bar{c}$	$q\bar{q}(uds)$	ISR	$b\bar{b}$	$c\bar{c}$	$q\bar{q}(uds)$	ISR	$b\bar{b}$	$c\bar{c}$	$q\bar{q}(uds)$	ISR
0.96	63.8	63.8	63.4	0.9	68.0	67.7	67.2	0.9	68.1	67.8	67.2	0.9
	67.4	67.6	67.2	1.1	71.0	70.9	70.3	1.1	70.6	70.4	69.7	1.0
1.00	64.7	64.6	64.3	0.9	68.8	68.5	67.9	1.0	68.8	68.4	67.8	0.9
	68.3	68.5	68.1	1.1	71.8	71.7	71.1	1.1	71.3	71.0	70.4	1.0
1.05	66.0	65.9	65.5	1.0	69.8	69.5	68.9	1.0	69.7	69.4	68.8	1.0
	69.6	69.8	69.4	1.2	72.9	72.7	72.2	1.2	72.2	72.0	71.4	1.1

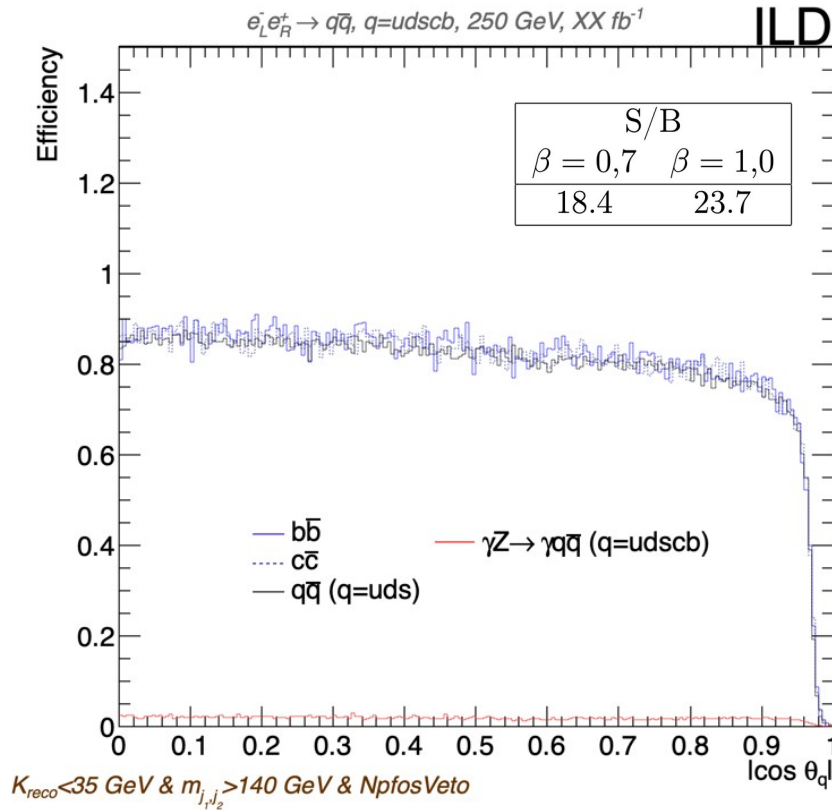
Table E3: Total efficiency of the preselection for the different quark flavors and radiative return for different values of R and  $\gamma$ . The second row of each set is constrained to the barrel region (for  $|\cos\theta| < 0.9$ )

The best parameter choices are R= 0.96 or 1 (in global efficiency estimation) and  $\gamma=0$  (due to the loss of efficiency in the forward/backward regions for other values)

R	Signal/Background		
	$\gamma = 0$	$\gamma = 0.5$	$\gamma = 1.0$
0.96	24.9	25.2	26.6
	29.4	27.6	27.8
1.00	23.7	24.5	25.7
	28.1	26.9	27.1
1.05	22.2	23.4	24.5
	26.6	25.9	26.0

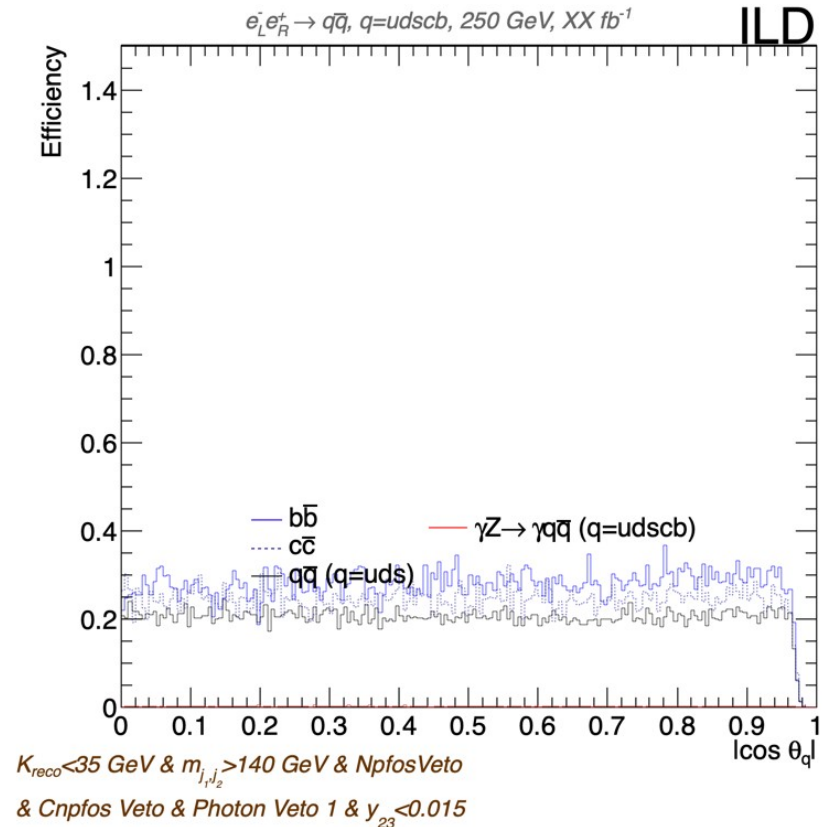
Table E4: S/B for the different quark flavors and radiative return for different values of R and  $\gamma$ . The second row of each set is constrained to the barrel region (for  $|\cos\theta| < 0.9$ )

# Re-optimization of the cuts: VLC algorithm – $\beta$ (E. I)



$\& \ C_{npfos} \ Veto \ \& \ Photon \ Veto \ 1 \ \& \ y_{23} < 0.015$

Fig. E3: Efficiency of the preselection for the different quark flavors (b,c, uds) vs the angular distribution of the two jet system (new samples, final configuration) for different  $\beta$  values: 0.7 (left) and 1.4 (right)



Lower values of  $\beta$  result in a lower S/B due to leakage of ISR while higher values leads to lower efficiencies and differences between quark flavors. We decided to keep  $\beta=1$

# Preselection for all quark flavors (u,d,s,c,b)

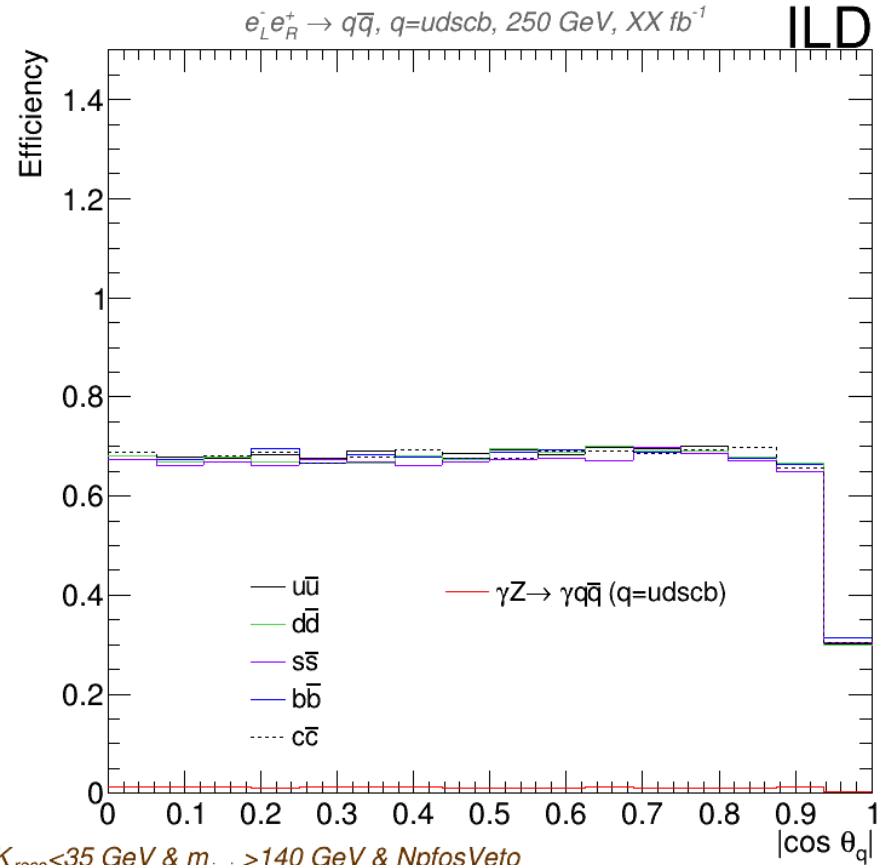


Fig. E4: Efficiency of the preselection for the different quark flavors (u,d,s,c,b) vs the angular distribution of the two jet system (new samples, final configuration)



# Efficiencies after each cut

Cuts:

- 1)  $K_{reco} < 35$  GeV
- 2)  $m_{2jets} > 140$  GeV
- 3) Charged N pfos
- 4) Photon veto
- 5)  $Y_{23} < 0.015$

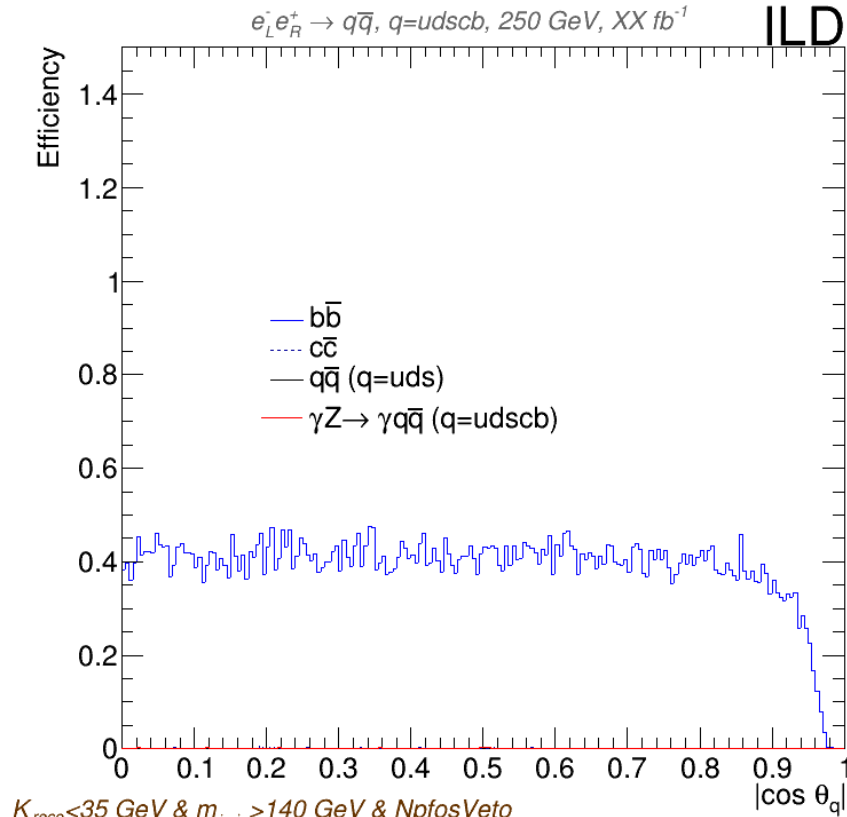
Cut	Efficiencies (%)				S/B
	$b\bar{b}$	$c\bar{c}$	$q\bar{q}$ (uds)	ISR	
1	81.2	80.8	81.0	5.7	4.9
2	80.9	80.7	81.0	5.2	5.4
3	80.9	80.7	81.0	5.2	8.4
4	77.9	77.3	76.5	1.5	18.4
5	64.7	64.6	64.3	0.9	23.7

Table E5: Selection efficiency, rejection power and Signal/Background ratio after each cut

Cut	Efficiencies (%)				S/B
	$b\bar{b}$	$c\bar{c}$	$q\bar{q}$ (uds)	ISR	
1	83.3	83.0	83.0	5.8	6.8
2	83.1	82.9	83.0	5.1	7.6
3	83.0	82.9	82.8	2.6	15.0
4	82.9	82.5	81.6	1.8	21.1
5	68.3	68.5	68.1	1.1	28.1

Table E6: Selection efficiency, rejection power and Signal/Background ratio after each cut. Data constrained to  $|\cos\theta| < 0.9$

# B-tagging



$K_{reco} < 35 \text{ GeV} \ \& \ m_{j_1, j_2} > 140 \text{ GeV} \ \& \ N_{pfosVeto}$

$\& \ C_{npfosVeto} \ \& \ PhotonVeto \ 1 \ \& \ y_{23} < 0.015 \ \& \ B\text{-tag}$

Fig. E5: Efficiency of the preselection for different quark flavors and ISR vs the angular distribution of the two jet system after applying b-tagging

Efficiencies (%)				S/B
$b\bar{b}$	$c\bar{c}$	$q\bar{q}$ (uds)	ISR	
37.51	0.02	0.00	0.06	35.34
40.80	0.02	0.00	0.08	40.49

Table E7: Total efficiency of the preselection for the different quark flavors and radiative return after applying b-tagging. The second row is constrained to  $|\cos\theta| < 0.9$

$e_L^- e_R^+ \rightarrow q\bar{q}$ ,  $q=udsbc$ , 250 GeV,  $XX \text{ fb}^{-1}$

ILD

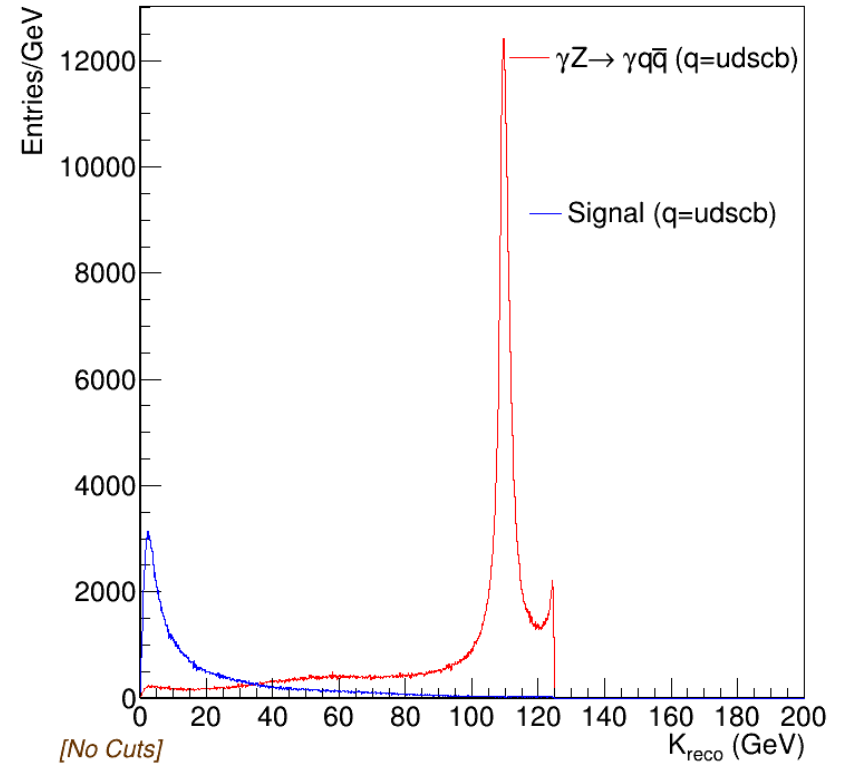


Fig. E6: Distribution of events vs  $K_{\text{reco}}$  for the reconstructed data with the Durham algorithm (left) and the VLC algorithm (right)

# Durham algorithm (II)

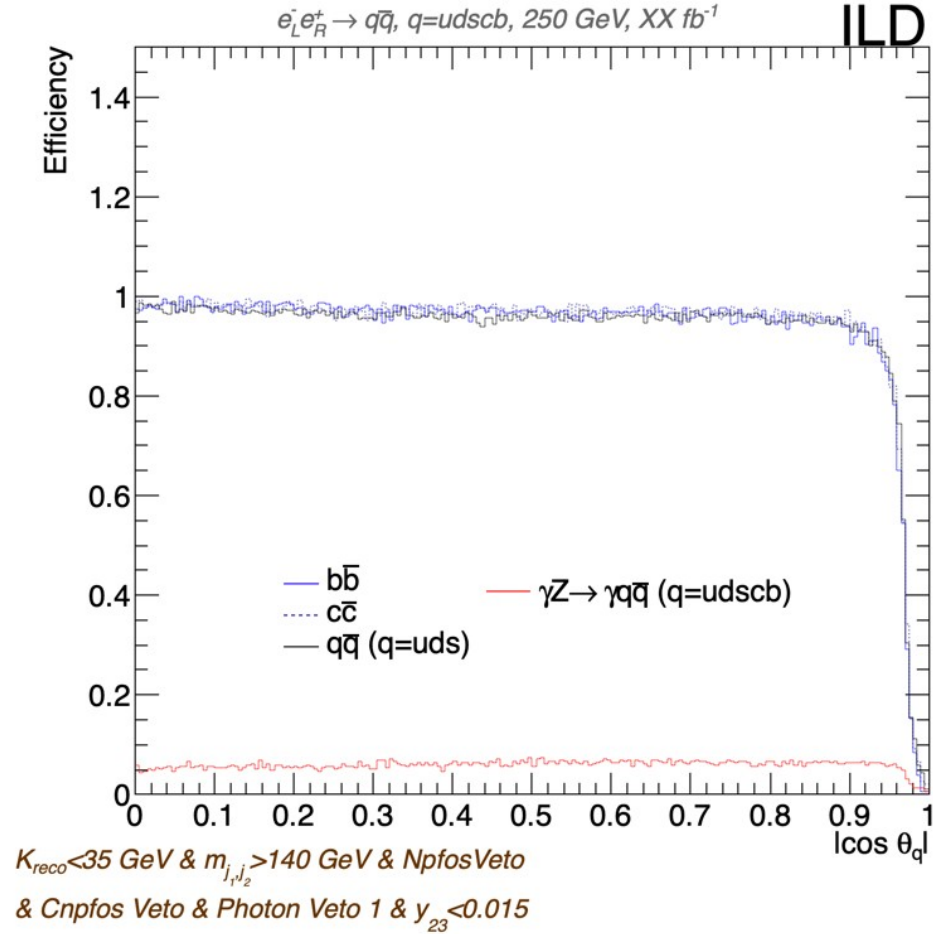


Fig. E7: Efficiency of the preselection for the different quark flavors (b,c,uds) vs the angular distribution of the two jet system (new samples, final configuration)

Efficiencies (%)				S/B
$b\bar{b}$	$c\bar{c}$	$q\bar{q}$ (uds)	ISR	
91.5	91.8	91.1	5.3	6.1
96.7	97.0	96.0	6.2	7.4

Table E8: Selection efficiency, rejection power and Signal/Background ratio after performing all cuts with the data reconstructed using the Durham algorithm